Ain Shams Engineering Journal 14 (2023) 101841

Contents lists available at ScienceDirect

Ain Shams Engineering Journal

journal homepage: www.sciencedirect.com

The research about application of quasi-zero stiffness vibration isolation technology in a large vehicle-mounted optic-electronic equipment

Zhaobing Chen [a,*], Shuaibei Yu [b], Bing Wang [a], Xinyu Zhuang [a], Feng Lin [a]

[a] Changchun Institute of Optics, Fine Mechanics and Physics, Chinese Academy of Science, Changchun, Jilin Province,130033, China
[b] The 52nd Research Institute, China Electronics Technology Group Corporation, Hangzhou, Zhejiang Province, 310000, China

ARTICLE INFO

Article history:
Received 8 March 2022
Revised 24 April 2022
Accepted 25 May 2022
Available online 09 June 2022

Keywords:
Truck-borne equipment
Photoelectric system
Zero-stiffness vibration isolation
Tracking bandwidth
Vibration suppression

ABSTRACT

The large vehicle-borne optic-electronic tracking equipment has the characteristics of heavy inertia, complex road condition and wide vibration spectrum. In order to solve the problem of passive broadband vibration isolation for vehicle-mounted moving platform optic-electronic equipment, a combined quasi-zero stiffness vibration isolation scheme is proposed. The vibration of the engine, generator, water cooler and the remaining vibration amplitude, frequency and Yaw of the road after passing the self-vibration isolation system of the vehicle are collected and confirmed by means of calculation simulation and field test. At the same time, the effective load of photoelectric equipment is analyzed by frequency sweeping test, and the corresponding multi-mode frequency points are obtained. According to the characteristics of the special equipment, a quasi-zero-stiffness vibration isolation system is designed to suppress the wide-frequency and high-amplitude vibration and Yaw caused by vehicle-borne vibration source, ground vibration source and resonance point of the equipment, the foundation stability of load equipment under dynamic condition is realized, which provides a condition for solving the problem of high precision and stability tracking which is greatly influenced by vibration. The vibration isolation system can realize the vibration isolation efficiency of 90% in the range of 20 Hz to 2000 Hz under the condition of 60 Km/h three-class highway with 1.5 t photoelectric load, and restrain the deflection caused by unbalance torque and vibration source offset effectively. It can be concluded that the quasi-zero stiffness vibration reduction and isolation combination design can effectively suppress the vibration of the large-scale vehicle-mounted optic-electronic equipment under the condition of moving platform.

1. Introduction

Inter travel stable tracking is one of the key technologies to be realized in the field of photoelectric tracking and photoelectric countermeasure [1–2]. Large vehicle mounted photoelectric equipment has large volume, high stiffness and strength requirements, complex pavement vibration spectrum and many and miscellaneous vehicle vibration excitation sources. The traditional passive vibration isolation scheme is difficult to effectively filter the vibration in low frequency band, and has no power to the unbalanced deflection caused by vibration and complex structure of equipment [3–5]. However, the active vibration isolation and damping scheme has some problems, such as large volume and difficult to accept weight. Therefore, both traditional passive vibration isolation and active vibration isolation are difficult to meet the high-precision and stable tracking requirements of large vehicle mounted photoelectric equipment under the current moving platform conditions [6–10].

Combined with the high-precision tracking and aiming requirements of vehicle mounted photoelectric equipment in a photoelectric countermeasure field, this paper analyzes the vibration isolation and damping characteristics of the equipment under dynamic conditions, analyzes the vehicle excitation source and road excitation source, and determines the vibration isolation and damping requirements of the equipment. Combined with the application background and technical and tactical indexes of the equipment, the vibration isolation and vibration reduction scheme

* Corresponding author.
E-mail address: chenzhaobing2010@163.com (Z. Chen).

Peer review under responsibility of Ain Shams University.

Production and hosting by Elsevier

https://doi.org/10.1016/j.asej.2022.101841
2090-4479/

based on passive quasi zero stiffness vibration isolator and supplemented by passive double shock absorber is selected. Combined with engineering experience, the simulation analysis results are designed, processed and combined, and the design scheme is verified by actual pavement test. After multiple rounds of improvement, the vibration isolation and damping combination system can effectively filter the vibration above 20 Hz. On this basis, the photoelectric equipment can effectively suppress the external excitation above 20 Hz through the compound axis tracking mode, and then realize the micro arc tracking accuracy of the photoelectric equipment to the target under the condition of moving platform. The vibration isolation equipment studied in this paper can achieve 80% vibration efficiency for the system random disturbance above 20 Hz in the position of the photoelectric window which easily causes amplification. This effect is relative to 80% isolation efficiency at the current isolation point.

2. Vibration reduction characteristics of large vehicle mounted photoelectric equipment during traveling

2.1. Excitation characteristics of vehicle related vibration sources

The vehicle adopts Dongfeng 10t chassis, the specific model is eq2102gj, the engine model is eq6bt5.9, and the displacement is 5.88l. Vehicle vibration sources mainly include three parts: engine, generator and water cooler. The vehicle chassis itself adopts leaf spring for primary vibration isolation. In order to test the excitation characteristics of the vehicle's own vibration source, a vibration acceleration test site is built, as shown in Fig. 1.

The vibration generated by the generator and water cooler of the vehicle is much smaller than that of the vehicle engine. Therefore, the final transmission test method is adopted for the two vibration tests, that is, the measurement is carried out at the installation structure of the photoelectric equipment. The absolute vibration of itself is not considered, but the vibration transmission of the two accessory vibration sources to the payload mounting surface is concerned. Fig. 2 shows the appearance and location of the generator and engine used in the project supported by this paper.

After testing, the excitation of the vehicle engine is mainly concentrated at about 37hz when the engine idles from 700 to 800 rpm, and has a great impact on the inclination vibration of the photoelectric system. When the engine runs above 800 rpm, the vibration acceleration at 37hz frequency is still the largest, but its impact on the inclination vibration of the photoelectric system decreases sharply. The vibration acceleration of generator and water cooler is one order of magnitude smaller than that of engine,

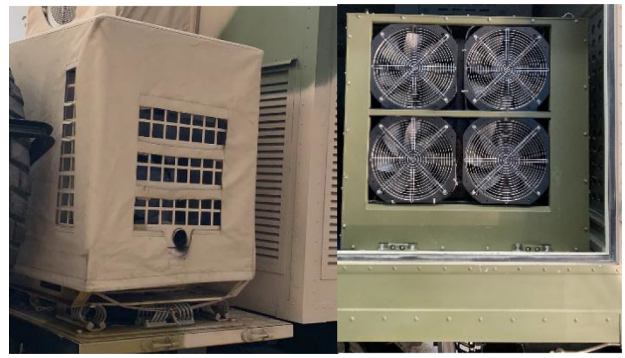

Fig. 2. Appearance of on-board generator and water cooler.

so the vibration influence of engine can be mainly considered in the subsequent vibration isolation design.

2.2. Excitation characteristics of pavement vibration sources

The road excitation is related to the characteristics of the road and the type and motion characteristics of the vehicle. The project supported by this paper adopts the requirements for vehicle body vibration in gjb150-1–86 military equipment environmental test method, and its vibration signal power spectral density is shown in Fig. 3 [11–15].

Because the project supported by this paper has a large vehicle volume, it is impossible to test its own characteristics in the form of shaking table. Therefore, the test conditions in the project are directly decomposed, and it is considered that the response results of the vehicle to the pavement can be tested under the conditions of moving forward and turning at the speed of 60 km / h on the pavement of class III Highway. The vibration characteristics of the road excitation acting on the load-bearing components of the photoelectric tracking system are measured by accelerometer, and the test diagram is shown in Fig. 4.

During the driving of the vehicle, the acceleration of the optical platform carrying photoelectric equipment is tested, mainly including the acceleration in three axis directions and the vertical acceleration at the left, right and front and rear maximum span positions of the platform. After testing, the engine vibration and road excitation vibration play a major role in the unbalanced torque vibration borne by the vehicle on the road, such as engine vibration, generator vibration, water cooler vibration, road excitation vibration and personnel walking. When the road surface is relatively flat, the vibration of the engine plays a major role in the

Fig. 1. Schematic diagram of on-board engine vibration source test site.

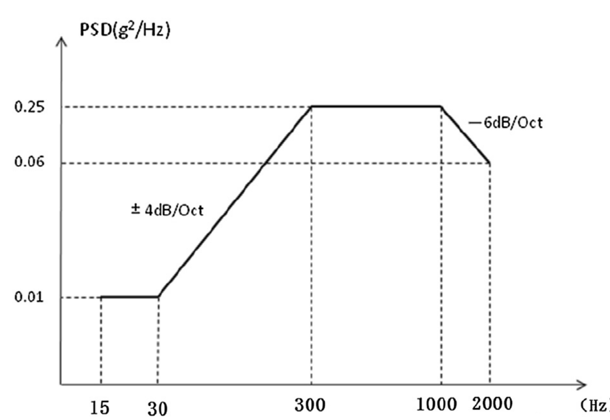

Fig. 3. Road vibration spectrum.

Fig. 4. Schematic diagram of vehicle road excitation test.

high frequency. When the road surface is uneven, the bump of the road surface has a greater impact on the optical platform. The instantaneous acceleration is one order of magnitude higher than the vibration acceleration of the engine, and the vibration amplitude is also very large, but this vibration is mainly concentrated in the low frequency band. The unbalanced amplitude in the left and right directions during vehicle driving is random, and the average acceleration on both sides is basically the same over a period of time. The acceleration and vibration amplitude in the front and rear directions of the optical platform are quite different, showing a trend of large in the rear and small in the front, which is very fatal for the photoelectric system which is difficult to tolerate the rapid change of small angle. Therefore, the inconsistency of vibration in different directions should be fully considered in the design of vibration isolation system.

2.3. Spectrum and deformation characteristics of photoelectric equipment

The tracking accuracy of photoelectric equipment depends on the corresponding speed of equipment hardware, the suppression of external disturbance, the servo control of resonance point of its own structure, the suppression of deformation of bearing point of photoelectric equipment and so on. The spectrum characteristics of the equipment itself are the characteristics of the photoelectric system itself. The corresponding characteristics can be determined by finite element simulation or frequency sweep vibration of the equipment itself. The equipment characteristics obtained by the frequency sweeping method have real reliability, but the equipment needs to complete the assembly of all parts and may cause damage to the equipment. Therefore, the frequency spectrum characteristics of photoelectric equipment are determined by finite element simulation in this paper. The bearing point of photoelectric equipment is the key point of the system. It is necessary to ensure that the point has sufficient stiffness strength and damping capacity when disturbed by the outside world, in order to achieve the minimum unbalanced deformation of the key point. The deformation of photoelectric equipment bearing point is very small, and the traditional measurement is difficult to accurately detect the deformation of micron scale. In this paper, the deformation of key points is analyzed by finite element simulation.

Firstly, simplify the system model, establish the finite element modal grid, conduct simulation analysis, and obtain the first-order modes of the structure, among which the first-order and second-order modes with the greatest impact are shown in the figure below. Fig. 5 and Fig. 6 show the first-order and second-order resonant frequencies of the equipment respectively.

The first two modes with the greatest influence are 52 Hz and 54 Hz respectively.

According to the practical application, the finite element model of the transition seat, the bearing part of the key optical system, is established, as shown in Fig. 7. Four support surfaces on the bot-

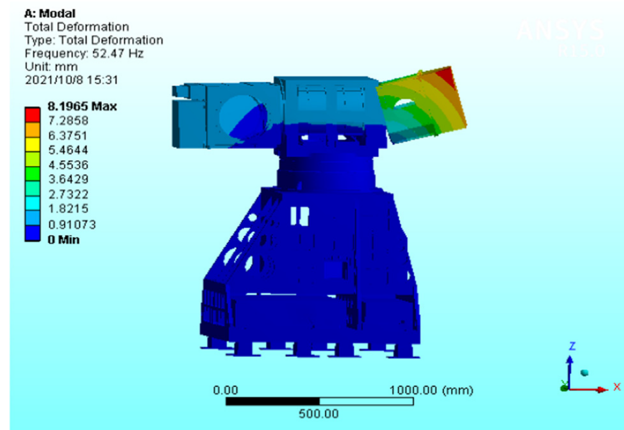

Fig. 5. First order mode.

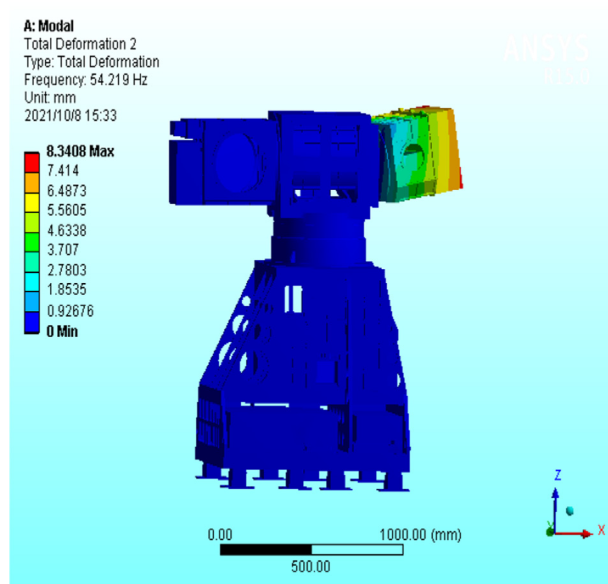

Fig. 6. Second order mode.

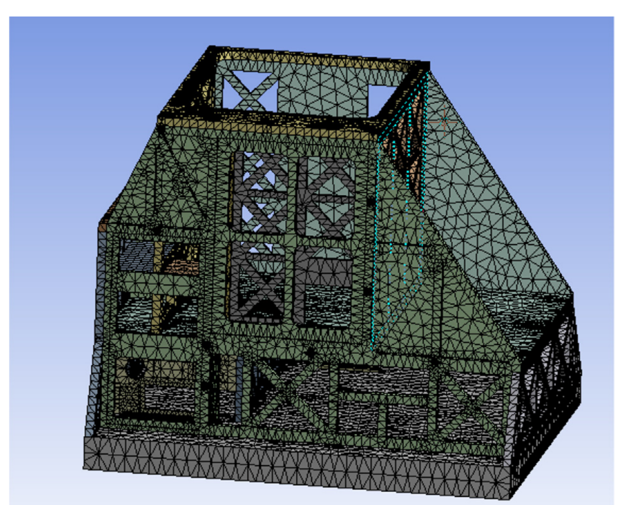

Fig. 7. Finite element model of point deformation.

tom surface are constrained, and random excitation is applied on the constraint surface. The boundary conditions of external vibration input are shown in Fig. 8.

The optical system adopts three-point positioning bearing, which are defined as three points a, B and C respectively. The maximum deformation of three points is obtained by inputting the above vibration conditions to the model. This paper takes the vertical direction with the greatest influence as an example. It is calculated that the maximum deformation variable at a is 0.12339 mm and the maximum stress value is 10.05mpa, as shown in Fig. 9 and Fig. 10.

The same method is used to obtain the stress–strain results of points B and C. The maximum deformation of point B in the vertical direction is 0.11594 mm, and the maximum stress value is 7.375mpa. The maximum deformation of point C in the vertical direction is 0.05227 mm, and the maximum stress value is 3.472mpa. According to the absolute strain value and position relationship of the three points, it can be calculated that the vertical angle change caused by external disturbance is mainly reflected in points A and C, and the maximum angle deformation is (0.12339–0.05227) / 0.6 = 0.1185mrad. The modal simulation of the whole tracking frame structure shows that the first-order and second-order modes that have the greatest impact on tracking are 52 Hz and 54 Hz respectively. According to the above simulation results, the deflection angle between point A and point C and the control of key points of system mode should be considered in the design of vibration isolator.

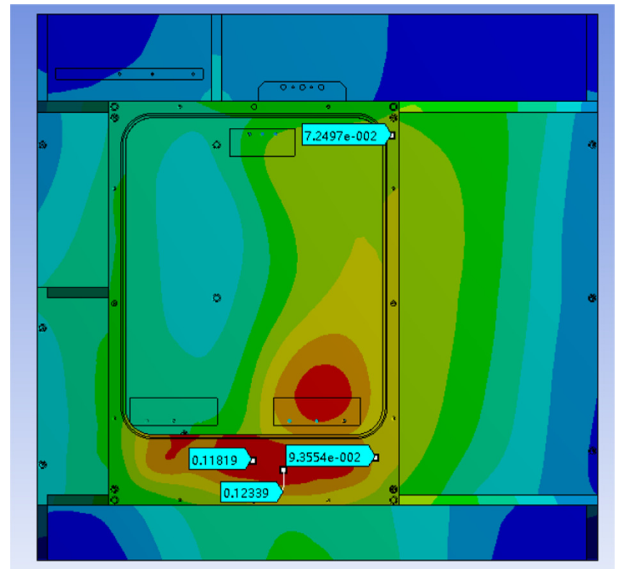

Fig. 9. Cloud diagram of plane deformation.

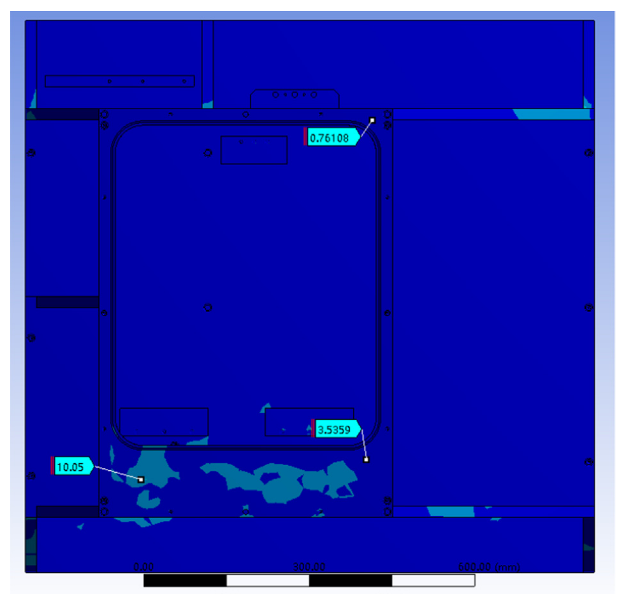

Fig. 10. Plane stress echogram.

3. Principle and application design of quasi zero stiffness vibration isolation and damping

In order to reduce the impact of wide-spectrum vibration, large angular velocity/large angular acceleration motion, unbalanced torque of the system itself and resonance point mode during vehicle traveling, the shock absorber is reasonably designed according to the above vehicle dynamic tracking boundary conditions and loading prototype parameters (engine, generator, water cooler, pavement and its own volume, weight, center of gravity, mode, etc.), Filter out the high-frequency and low amplitude vibration of the vehicle platform. The reasonable design of vibration isolator is the premise to realize the stable and dynamic tracking of the system, suppress the high-frequency vibration of the system as far as possible, and hand over the low-frequency vibration part to the servo system. The performance of vibration isolator to suppress high-frequency vibration components determines the system bandwidth. The integrated vibration isolation technology mainly includes the research on equipment vibration isolation and equipment vibration reduction. The equipment vibration isolation is mainly to set a vibration isolation system between the tracking and launching turntable and the vehicle carrying platform. Based on the above analysis results, a quasi zero stiffness isolator which can meet the above boundary conditions is designed to isolate the equipment. The design objective of vibration isolation is that the attenuation rate above 25 Hz shall reach more than 90%, and the angular velocity of external disturbance attached to the tracking axis after vibration isolation shall not be greater than 10°/s.

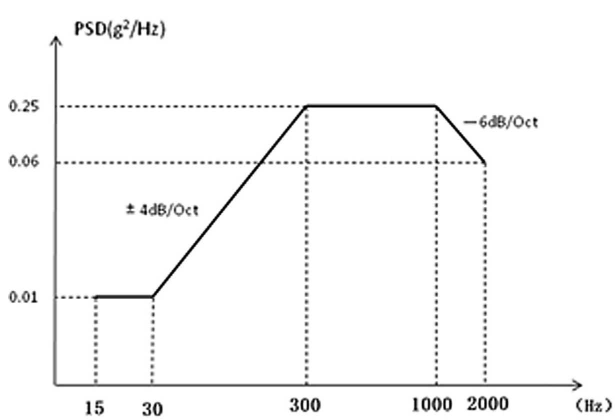

Fig. 8. Input curve of external vibration boundary conditions.

3.1. Quasi zero stiffness vibration isolation principle

The vehicle vibration on the road is mainly low-frequency and ultra-low-frequency vibration distributed between 3 Hz and 100 Hz. However, the traditional vibration isolation technology generally has problems such as high cost, high initial vibration isolation frequency and resonance. Starting from the demand of high-precision tracking and aiming of large-scale vehicle photoelectric system on the road, the design of an ultra-stable platform with low-frequency and ultra-low frequency vibration isolation characteristics and effectively overcoming unbalanced torque and multi-point resonance point suppression is the main content of this paper.

The traditional vibration isolation system is mostly linear vibration isolation system, which is mostly composed of springs and dampers. Its principle is shown in Fig. 11. If acceleration excitation is applied to the base, the motion equation of the system is [16–17]:

Mx + cx + kx = mpsinθt (1).

The amplitude B of the isolated equipment is:

$$B = a\sqrt{\frac{1+(2\zeta\omega/\omega_n)^2}{\left[1-(\omega/\omega_n)^2\right]^2+(2\zeta\omega/\omega_n)^2}} \tag{2}$$

Absolute transmissivity is defined, which means the ratio of the vibration amplitude of the supporting equipment transmitted to the equipment through the vibration isolator to the displacement amplitude acting on the object without the vibration isolator, that is:

$$\beta = \frac{B}{a} = \sqrt{\frac{1+(2\zeta\omega/\omega_n)^2}{\left[1-(\omega/\omega_n)^2\right]^2+(2\zeta\omega/\omega_n)^2}} \tag{3}$$

According to the above formula$\lambda = \frac{\omega}{\omega_n}$, the curve with can be obtained, as shown in Fig. 12.

3.2. Quasi zero stiffness vibration isolation design

The quasi zero stiffness vibration isolation system discussed in this paper is installed on the equipment base, as shown in Fig. 13. The designed quasi zero stiffness vibration isolator is arranged at the bottom of the equipment according to the principle that the total torque of the equipment is zero and based on the center line of the equipment. The quantity configuration, software and hardware settings of vibration isolators are carried out according to the above simulation and test results.

The quasi zero stiffness isolator is composed of many negative stiffness elements, and each negative stiffness element can be simplified, as shown in Fig. 14. Its stiffness can be expressed as:

k(x) = dF dx = ω02(1-a2(x2 + α2)) (4)

The stiffness curve of the negative stiffness element is shown in Fig. 15. The stiffness of the quasi zero stiffness system at the equilibrium point is 0, the corresponding restoring force is 0, and the restoring force at other positions is not 0; The more away from the equilibrium position, the faster the change rate of the restoring force; Within a certain range near the equilibrium position, the restoring force is very small, close to 0. Therefore, as long as the load range of the vibration isolator is reasonably set, the transmission rate of vibration can be well controlled.

Passive vibration isolation is to reduce the vibration transmitted from the foundation to the object. Therefore, the effect of vibration isolation can be measured by the ratio of object vibration to foundation vibration. In this paper, the ratio of object vibration amplitude to excitation amplitude is defined as the transmission rate of the vibration isolation system. The greater the transmission rate, the worse the vibration isolation effect. Based on this, the effects

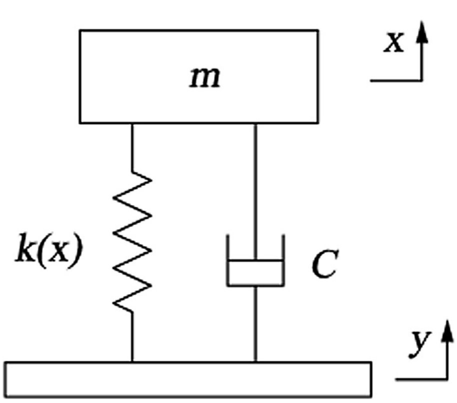

Fig. 11. Schematic diagram of vibration isolation system.

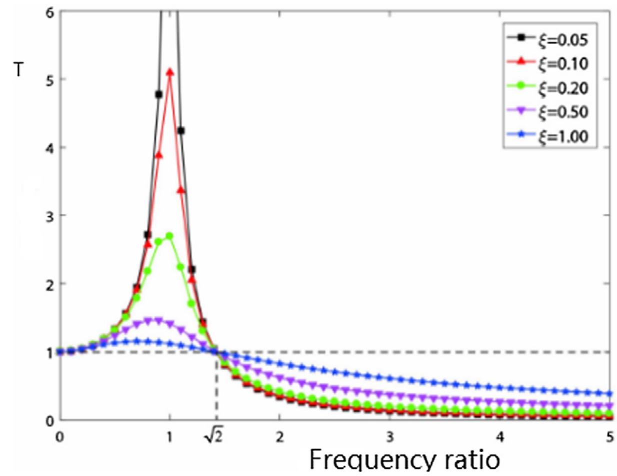

Fig. 12. Transmissibility curve of linear passive vibration isolation system.

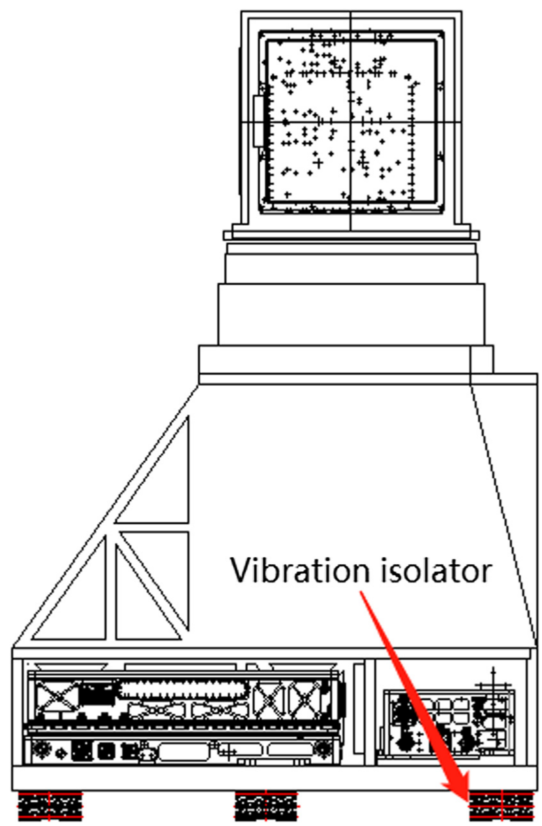

Fig. 13. Setting position of quasi zero stiffness isolator.

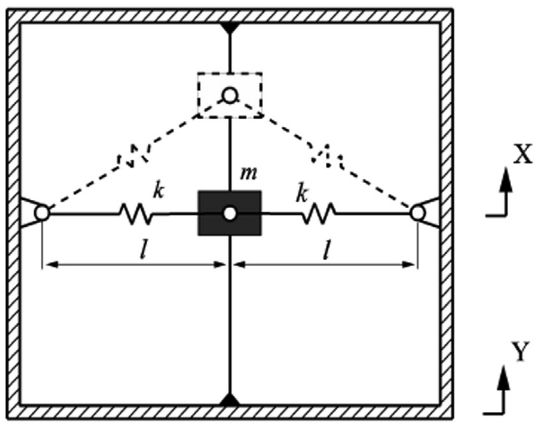

Fig. 14. Negative stiffness element.

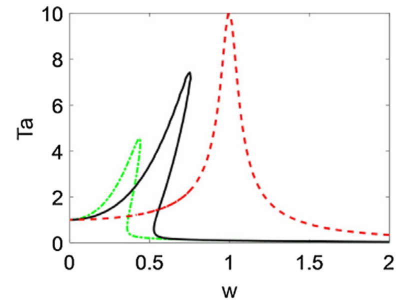

Fig. 16. Acceleration transfer rate of quasi zero stiffness element.

of different excitation amplitude and damping ratio on the displacement transmission rate and acceleration transmission rate of the vibration isolation system are investigated respectively. Through simulation analysis, the transmission rate of quasi zero stiffness element is shown in Fig. 16. The red line is the transmission rate of other vibration isolation systems, and the green line is the transmission rate of zero stiffness vibration isolation. It can be seen that the use of quasi zero stiffness structure can reduce the vibration isolation cut-off frequency and improve the high-frequency vibration isolation efficiency.

Based on the above design principles, a quasi-zero stiffness finite element model is established. According to the engine, generator, water cooler, road excitation of the system vehicle, the resonance frequency of the equipment itself and the unbalanced deformation conditions after impact, combined with previous engineering experience, a set of vibration isolation system is designed. The system is composed of two groups of eight vibration isolators, the layout position is set according to the above excitation and unbalance torque and the theoretical center of gravity position of the system. The vibration isolation capacity of each vibration isolator is different. In order to verify whether the vibration isolation system meets the requirements, it is necessary to simulate and verify the vibration isolation capacity and combined vibration isolation capacity of each vibration isolator. In this paper, the vibration isolation design of No. 1 vibration isolator is simulated as an example. Impose fixed constraints on the lower end face of No. 1 vibration isolator, apply load on the upper end face, set the excitation frequency as 0-1000hz sweep excitation, set the acceleration value as 50 M / S2, and the location of the measuring points is shown in Fig. 17. The response curves of point a point B are obtained through calculation, as shown in Fig. 18 and Fig. 19.

By analyzing the response results of the vibration isolator before and after vibration isolation, see whether the vibration isolator meets the requirements of the vibration isolation efficiency and capacity allocated to the vibration isolator by the vibration isolation system. If not, adjust the structural parameters of the vibration isolator until it meets the requirements of the system for its software and hardware. As shown in Figs. 18 and 19, the No. 1 vibration isolator can meet the design requirements of the system for vibration isolation at this point. This simulation analysis method is also used to evaluate the vibration isolator system, guide the practice with theory, and process the vibration isolation system according to the final optimization results.

4. Test and analysis of quasi zero stiffness vibration isolation system

The quasi zero stiffness vibration isolation system discussed in this paper is analyzed by single machine test and system test. The method of single machine test is to install the vibration isolator on the optical machine system under test, put the system on the vibration table for frequency sweeping vibration, test the acceleration values at different positions, and obtain the vibration isolation efficiency of the system. The system test method is to install the vibration isolator and photoelectric equipment on the vehicle, configure accelerometers at the positions before and after vibration isolation, drive the vehicle carrying large photoelectric equipment under actual road conditions, test the values of each accelerometer,

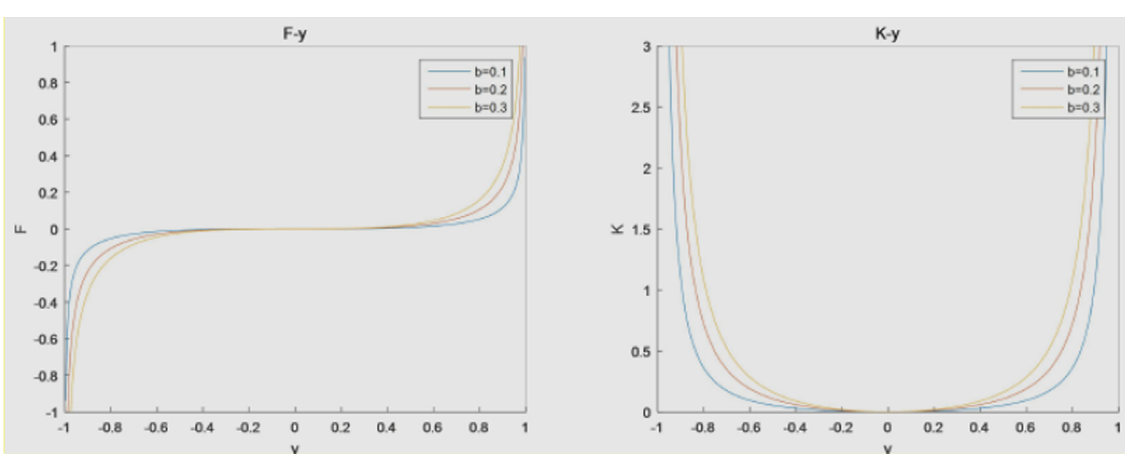

Fig. 15. Stiffness curve and force transfer curve of negative stiffness element.

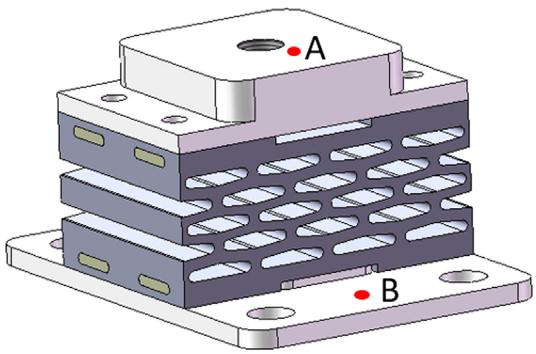

Fig. 17. location of measuring points.

and analyze to confirm whether the vibration isolation system can meet the vibration isolation design requirements. Fig. 20 shows a large photoelectric device located on the shaking table. Fig. 21 shows the combination of vibration isolation and damping effects in three directions at a certain position after vibration isolation of the vibration isolator when the vibration table is swept at the frequency of 0 ~ 2000 Hz.

It can be seen from Fig. 21 that when the frequency is swept above 20 Hz, the vibration isolator can achieve more than 90% vibration isolation efficiency, in which the vibration isolation efficiency in X and Y directions is higher, while the vibration isolation effect in Z direction in vertical direction is the worst, and there is an upward trend in multiple frequency bands. These points are basically consistent with the modal analysis results of the system. Swept frequency vibration can see the overall vibration isolation effect of the vibration isolation system, but it can only indirectly explain the actual vibration isolation effect of the system. Therefore, on the basis of swept frequency verification, this paper verifies the vibration isolation efficiency of the system by organizing

Fig. 20. Vibration isolation efficiency and frequency sweep site of photoelectric equipment.

field tests. Fig. 22 shows the state of photoelectric equipment after loading.

Install the accelerometer at the upper and lower positions of the vibration isolator, let the vehicle drive normally on class III Highway, test the acceleration values at different positions, compare and analyze the data, fit the vibration curve, and confirm whether the set of vibration isolation system meets the designed vibration isolation efficiency. Taking test points 1, 2 and 3 as examples, the three points are the vertical direction of the vehicle girder, the vertical direction of the lower part of the vibration isolator and the vertical direction of the upper part of the vibration isolator, as shown in Fig. 23.

The idle speed of the vehicle has a lot of influence on the system. In order to verify the vibration isolation effect of the

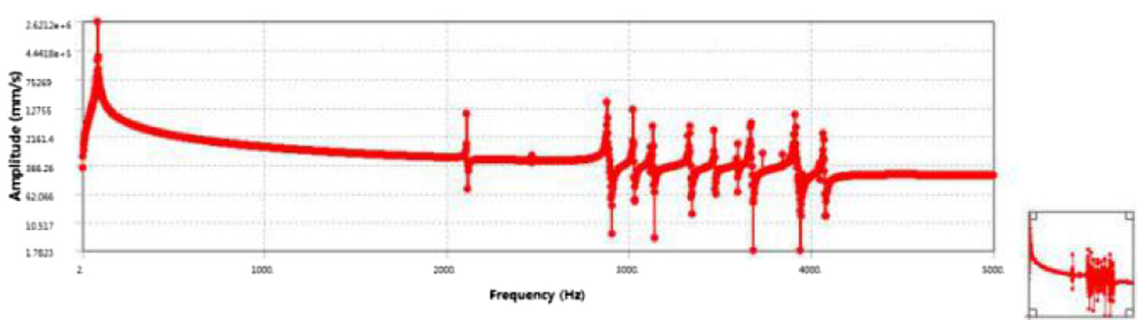

Fig. 18. Response curve at A.

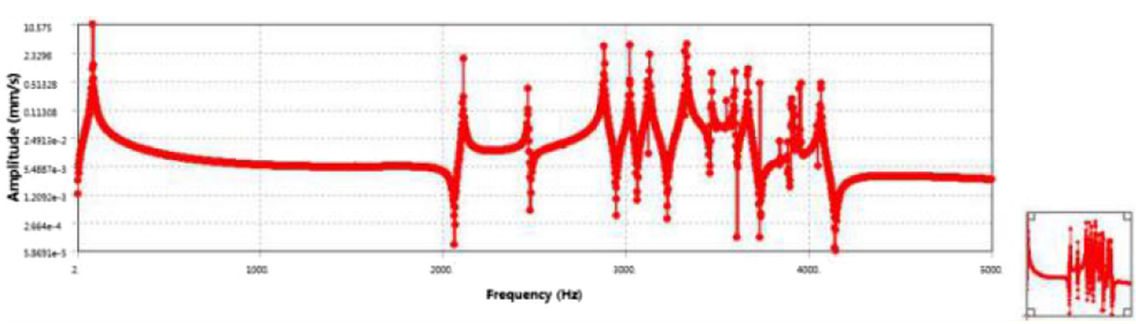

Fig. 19. Response curve at B.

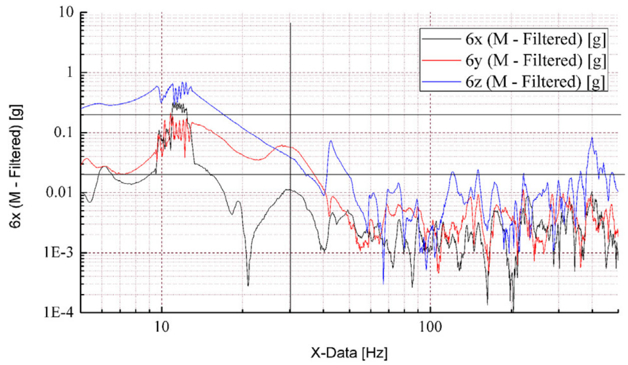

Fig. 21. Three direction frequency sweep vibration isolation efficiency of equipment.

Fig. 22. Loading test diagram of photoelectric equipment.

Fig. 23. Schematic diagram of test points for system vibration isolation efficiency test.

vibration isolation system on the engine idle vibration, the engine idle vibration isolation efficiency test is carried out separately. Take measuring point 1 and measuring point 3 for analysis. The green curve in Fig. 23 is the vibration acceleration curve of measuring point 1, and the red curve is the vibration acceleration curve of measuring point 3. After installing vibration isolators at different speeds, the vibration transmission rate can be reduced by more than 90%, and the higher the speed, the more.

The traveling test is the final test of the system. The test is also analyzed at measuring point 1 and measuring point 3. As shown in Fig. 24, the vibration transmission rate can be reduced by more than 90% at a constant speed of 20 km / H $\sim$ 60 km / h. Fig. 25 shows the vibration transmission rate above 20 Hz is reduced by 95.9%.

From the above test results, this set of quasi zero stiffness vibration isolation system can meet the vibration isolation requirements of photoelectric equipment under the conditions of engine vibration, generator vibration, water cooler vibration, road bumps, self-torque imbalance and so on, and realize a large proportion of vibration frequencies above 25 Hz.

5. Conclusion

Based on the working requirements of large-scale vehicle photoelectric equipment, this paper establishes the disturbance category and influence model of photoelectric system working on the road according to the requirements of high-precision tracking and aiming. At the same time, according to the characteristics of quasi zero stiffness vibration isolator, a vibration isolation system which can meet the requirements of the system is designed. The influencing factors of vibration are quantitatively analyzed by means of simulation analysis and practical test. According to the analysis results, eight two group matched vibration isolation systems are designed to meet the vibration isolation requirements of a large vehicle mounted photoelectric equipment. The vibration isolation efficiency of the vibration isolation system is quantitatively evaluated by means of shaking table frequency sweep and field sports car acceleration test. The results show that the vibration isolation system can achieve the vibration isolation efficiency of the photoelectric equipment above 20 Hz and above 90% under complex road conditions. This provides a solid foundation for the high-precision tracking of photoelectric equipment. The effective tracking of the target can be realized when the bandwidth of the tracking equipment meets more than 20 Hz. The lower limit vibration violation efficiency of the quasi-zero stiffness isolator is 20 Hz in low frequency range. To achieve a lower frequency partition, the

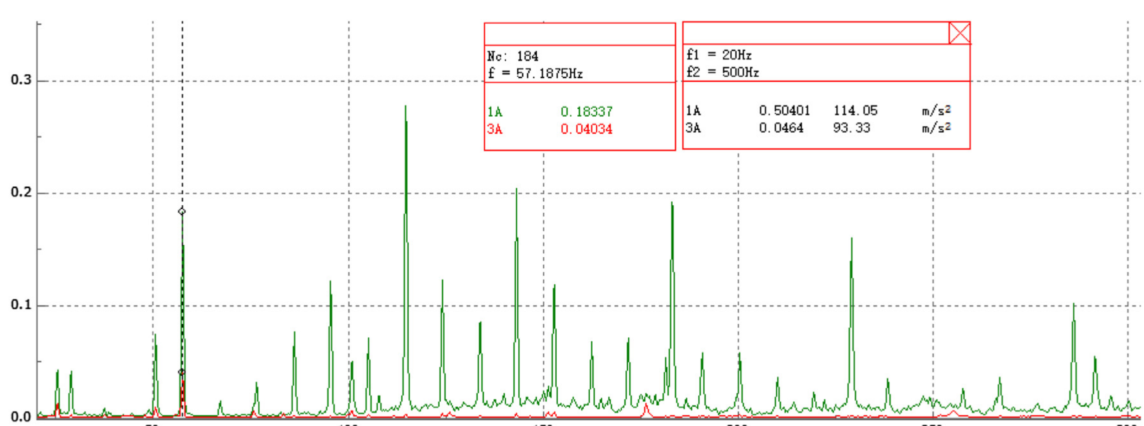

Fig. 24. Idling equipment fully open for 1000 revolutions (vibration transmission rate above 20 Hz is reduced by 90.8%).

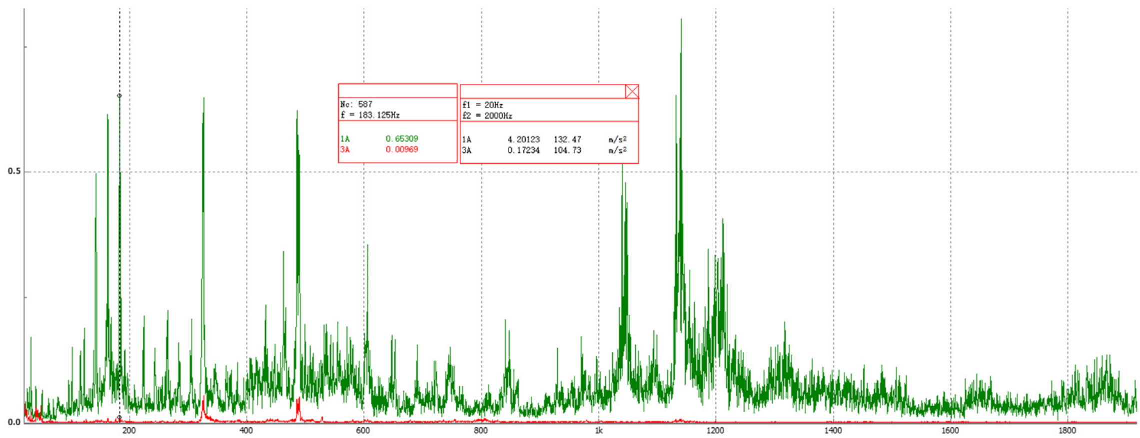

Fig. 25. The equipment is fully opened at a constant speed of 60 km / h.

effects of active vibration or active/passive vibration isolation equipment on optical system should be studied.

Declaration of Competing Interest

The authors declare that they have no known competing financial interests or personal relationships that could have appeared to influence the work reported in this paper.

References

[1] Junfeng Hu, Xingxing C. Optimal design of micro motion platform with zero stiffness. Optical precision engineering 2018;26(6):1430–40.
[2] Shuang LAN. Yang Xiaoxiang. Design and dynamic simulation of shear fork quasi zero stiffness vibration isolator. Mechanical design and research 2017;33 (2):20–4.
[3] Wen G, He J, Liu J, Lin Yu. Design, analysis and semi-active control of a quasi-zero stiffness vibration isolation system with six oblique springs. Nonlinear Dyn 2021;106(1):309–21.
[4] Zheng Y, Zhang X, Luo Y, Xie S, Zhang Y. Harnessing the compressed-spring mechanism for a six-degrees-of-freedom quasi-zero-stiffness vibration isolation platform. Journal of Vibration and ControlVolume 2021;27(15-16):1793–805.
[5] Lu SF, Jiang Y, Zhang W, Song XJ. Vibration suppression of cantilevered piezoelectric laminated composite rectangular plate subjected to aerodynamic force in hygrothermal environment. European Journal of Mechanics A-Solids 2020;83.
[6] Mingliang Wu, Chenming Z, Laixi Z. Research progress of quasi zero stiffness vibration control system. Journal of Nanjing University of technology 2021;45 (1):18–26.
[7] Lu SF, Li HJ, Zhang W, Song XJ. Vibration reduction of FG-CNTR piezoelectric laminated composite cantilever plate under aerodynamic load using full-dimensional state observer. Eng Struct 2022;255.
[8] Ying Jianyu. Passive suspension design based on quasi zero stiffness principle. Hangzhou: Zhejiang University, 2018.
[9] Chen J, Zhang W, Yao M, Liu J, Sun M. Vibration reduction in truss core sandwich plate with internal nonlinear energy sink. Compos Struct 2018;193:180–8.
[10] Chen JE, He W, Zhang W, Yao MH, Liu J, Sun M. Vibration suppression and higher branch responses of beam with parallel nonlinear energy sinks. Nonlinear Dyn 2018;91(2):885–904.
[11] Chen JE, Zhang W, Yao MH, Liu J. Vibration suppression for truss core sandwich beam based on principle of nonlinear targeted energy transfer. Compos Struct 2017;171:419–28.
[12] Cao H, Chang Y, Zhou J, Zhao X, Lu L, Chen F, et al. High-Efficiency Vibration Isolation for a Three-Phase Power Transformer by a Quasi-Zero-Stiffness Isolator. Shock Vib 2021;2021:1–11.
[13] Liu Y, Song C, Xu L, Ji W. Experimental study on dynamic characteristics of a quasi-zero stiffness vibration isolator. Journal of Physics: Conference SeriesVolume 2021;1732(1):012171.
[14] Wang Y, Li H-X, Cheng C, Ding Hu, Chen L-Q. Dynamic performance analysis of a mixed-connected inerter-based quasi-zero stiffness vibration isolator. Struct Control Health Monit 2020;27(10).
[15] Chen Z, Shi K, Chen N, Shi L, Zhuang X, Zhou J, et al. The experimental study about laser-induced dizziness effect of medium-wave infrared seeker which based on image processing. J Vis Commun Image R 2019;59:401–6.
[16] Chen Z, Chen N, Shi K, Li G, Liu X. The Research about High Dynamic and Low-gray Target Image Differential Capture Technology Based on Laser Active Detection. EURASIP Journal on Image and Video Processing 2018;2018(1).
[17] Chen Z-B, Li G-N, Liu X-Y, Liu X-Y. The structure form layout and installation design about car-based photonics mast. Discrete Mathematical Sciences Cryptography 2017;20(1):231–8.

Chen Zhaobing received the BS degree in Qingdao University, Qingdao, China, in 2005, the Ph.D degree in Mechanics from Changchun Institute of Optics, Fine Mechanics and Physics, Chinese Academy of Science, Changchun, China, in 2011. In 2008, he joined Changchun Institute of Optics, Fine Mechanics and Physics, Changchun, China. Before 2013, he was an assistant professor in Changchun Institute of Optics, Fine Mechanics and Physics. From 2013 to now, he is an associate professor of Changchun Institute of Optics, Fine Mechanics and Physics. His research interests include research on optical Mechatronics, image processing, laser echo technology research.

Yu Shuaibei was borned in Changchun, JiLin Province, Master, Associate professor,He worked in 52nd Research Institute,China Electronics Technology Group Corporation,graduated from Changchun University of Sciences and Technology in 2017,researched in aerial imaging and measurement technology.

Zhuang Xinyu was an assistant professor in Changchun Institute of Optics, Fine Mechanics and Physics. From 1999 to now, he is an associate professor of Changchun Institute of Optics, Fine Mechanics and Physics. His research interests include research on optical Mechatronics, laser echo technology research.

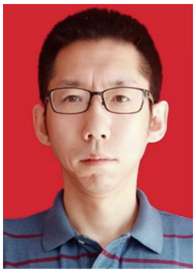

Wang Bing was an assistant professor in Changchun Institute of Optics, Fine Mechanics and Physics. He is an associate professor of Changchun Institute of Optics, Fine Mechanics and Physics. His research interests include research on optical Mechatronics, laser echo technology research.

Lin Feng from 2021 to now, he is a Research Intern of Changchun Institute of Optics, Fine Mechanics and Physics. His research interests include research on optical Mechatronics, laser echo technology research, image processing,structure design of precision machinery and optical system.